

Physical Properties of 6R-TaS₂

E. Figueroa,* Y.-K. Kuo,* A. Olinger,* M. A. Lloyd,† L. D. Bastin,† S. Petrotsatos,* Q. Chen,* B. Dobbs,* S. Dev,† J. P. Selegue,† L. E. DeLong,* C. P. Brock,† and J. W. Brill*.¹

*Departments of Physics and Astronomy and †Department of Chemistry, University of Kentucky, Lexington, Kentucky

Received December 17, 1993; in revised form May 26, 1994; accepted June 6, 1994

We have characterized powders of 6R-TaS₂ by means of (ac and dc) susceptibility, resistivity, and differential scanning calorimetry. Three phase transitions are observed below 350 K: a superconducting transition with its onset at 2.3 K and transitions (at 80 and 325 K) which involve increases in resistivity and decreases in susceptibility upon cooling. We suggest that the upper two transitions are charge-density-wave transitions; this identification is supported by the strong pressure dependence of the superconducting transition, $dT_c/dP = 0.18$ K/kbar. © 1995 Academic Press, Inc.

INTRODUCTION

TaS₂ is a prototype of a quasi-two-dimensional metal in which strongly bonded conducting layers are weakly bonded by van der Waals interactions (1). Because of the weak bonding between the layers, it is possible to intercalate a number of electropositive host species, from metal ions to large organic molecules, between the layers, thereby changing the conduction electron density and interlayer coupling (2, 3). Moreover, it is possible to prepare several polytypes of TaS₂, which differ in the stacking and/or structure of the layers (1). In this paper, we discuss the properties of 6R-TaS₂ (4). Although known for more than 30 years (4), this polytype has not been extensively characterized due to the difficulty in obtaining pure samples; the properties we measure differ somewhat from those previously reported (5).

In TaS₂ (1), close-packed layers of tantalum atoms are sandwiched between close-packed layers of sulfur atoms, with van der Waals bonds between neighboring sulfur layers. The Ta atoms may be in an octahedral or trigonal prismatic coordination with six S atoms. Polytypes differ in the alignment of sandwiches as well as in the coordination within a sandwich. For example, the coordination of each layer is octahedral in the 1T polytype, while in the 2H and 3R polytypes, all layers have trigonal prismatic coordination. In other polytypes, such as 4H_b and 6R, the octahedral and trigonal prismatic layers alternate (1).

¹ To whom correspondence should be addressed.

(In this "nA_x" notation, *n* = the number of layers/unit cell, *A* describes the symmetry of the unit cell, e.g., T = trigonal, H = hexagonal, and R = rhombohedral, and subscripts identify different structures with the same "nA".) In the 6R polytype, the stacking sequence is [AbA BcA BcB CaB CaC AbC], where upper (lower) case letters refer to sulfur (tantalum) atoms (6).

EXPERIMENTAL DETAILS

Two batches of TaS₂ were prepared by heating stoichiometric mixtures (total mass 3 g) of tantalum powder (99.98%) and sulfur (99.9995%) in evacuated 100 cm³ quartz tubes. The tubes were held at 1220 K for 8 days, then held at $T_A = 920$ K for 4 days, before slowly cooling to room temperature. The same temperatures, when used with tantalum foil as starting material, yields 2H-TaS₂ powder (1, 7); the octahedral and mixed-coordination polytypes are usually prepared at higher T_A (1). In the present case, the product was a flowing blue-black powder, similar in appearance to 2H-TaS₂. However, X-ray diffraction indicated that the layer spacing was 5.97 Å, equal to the spacing for 3R or 6R-TaS₂, and smaller than that for 2H-TaS₂ (6.03 Å) (1).

Because of their layered structure, X-ray diffraction patterns of TaS₂ powders are generally dominated by (00 l) reflections. To obtain a more random distribution of crystallite orientation, the ground powder was sprinkled onto sticky tape. The observed patterns for both growth tubes were identical; the pattern, shown in Fig. 1, is very similar to that expected for 6R-TaS₂ (1, 6), also shown in the figure. (The calculated pattern shown is for random crystallite orientation.) In contrast, the pattern is *qualitatively* different (i.e., has extra or missing lines) from that of *any* other known polytype, even after adjusting for slightly different layer spacings. However, a Rietveld fit of the structure, including preferred crystallite orientation, has quantitative differences with the observed pattern; in particular, the observed (101) line, indicated by the arrow in Fig. 1, is too strong. The fit cannot be significantly improved by including a mixture of any other known tanta-

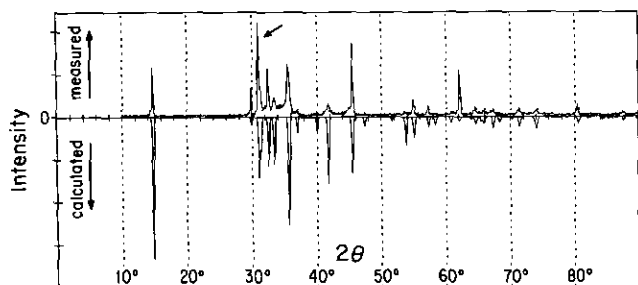


FIG. 1. Observed and calculated (6) X-ray diffraction powder pattern (with $\text{CuK}\alpha$ radiation) for 6R-TaS₂. The arrow indicates the (101) line.

lum sulfide (or oxide). The reasons for the discrepancy are not understood; perhaps the TaS₂ sandwiches in this polytype have lower symmetry than had been thought (1, 6). We conclude that the material is essentially single phase 6R-TaS₂, although we cannot rule out a slight off-stoichiometry or, as mentioned below, the presence of absorbed hydrogen.

The dc magnetic susceptibility of the powder was measured at 12 kG with a Faraday balance between 4.5 and 350 K. Results for samples from both growth tubes are shown in Fig. 2 and are very similar. Two large decreases in susceptibility are observed as the sample is cooled, with maxima at $T_1 = 325$ K and $T_2 = 80$ K. Very slow (<0.5 K/minute) temperature cycling indicated that the upper transition is slightly hysteretic, with $\Delta T_1 = 3$ K, as shown in the inset. We could not resolve any hysteresis ($\Delta T_2 < 2$ K) at the lower transition. Shoulders are observed in the susceptibility below both maxima (i.e., at 315 and 35 K). The susceptibility was independent of

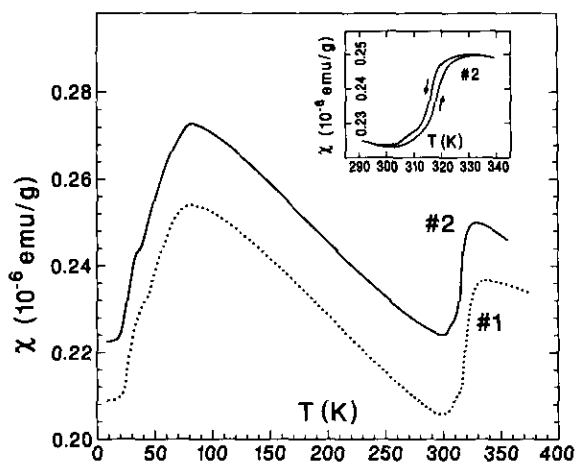


FIG. 2. Temperature dependence of dc magnetic susceptibility of samples from two growth tubes of 6R-TaS₂: dotted curve, growth-tube-1; solid curve, growth-tube-2. Inset: Results for sample 2 above room temperature. Temperatures were swept with $|dT/dt| < 0.5$ K/min; arrows indicate the directions of temperature sweeps.

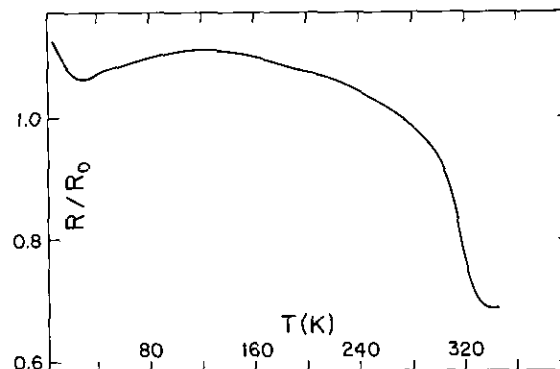


FIG. 3. Temperature dependence of resistance of a pellet from growth-tube-1, normalized to its room temperature value.

magnetic field for fields up to 12 kG at all temperatures. The small difference in the magnitude of the susceptibility for the two growth tubes presumably reflects different impurity concentrations, which may be the consequence of contamination on the quartz tubes.

We also measured the electrical resistances of pellets prepared from these powders. It is notoriously difficult to prepare pellets of transition metal dichalcogenides due to their "waxy" layered surfaces (7). We prepared a special dye, piston, and anvil that could withstand pressures as great as 10 kbar to prepare pellets of these materials. Results for a typical pellet are shown in Fig. 3. The results should only be considered qualitative because (i) the crystallites are highly aligned parallel to the pellet's pressed surface and although a 4-contact measurement was made, the contacts were not in an ideal 4-probe configuration; (ii) the large pressures used to prepare the pellet cause considerable strain in the crystallites; and (iii) the resistance of the pellet is probably dominated by interparticle resistances. Nonetheless, both transitions are clearly observed as resistance increases with decreasing temperature. The upper transition is at 320 K and the lower at 30 K; the depression of the lower transition from the temperature observed in susceptibility is presumably due to the large strains frozen into the pellet.

We investigated the T_1 transition with differential scanning calorimetry using a Perkin-Elmer DSC7 system. Samples from both growth tubes gave the same results. The differential heat flow, converted to an effective specific heat, c_{EFF} (8), is shown in Fig. 4. For a transition with a sharp latent heat, the width of the transition as observed with DSC should be proportional to $(dT/dt)^{1/2}$ (9); however, for our samples, the width of the anomaly was independent of sweep rate for rates ≤ 25 K/min. Thus the width of the observed anomaly is "intrinsic" to the sample; i.e., $c_{\text{EFF}} = c_p + dl/dT$, where c_p is the specific heat and l is the molar latent heat, assumed to be distributed over a finite temperature interval because of sam-

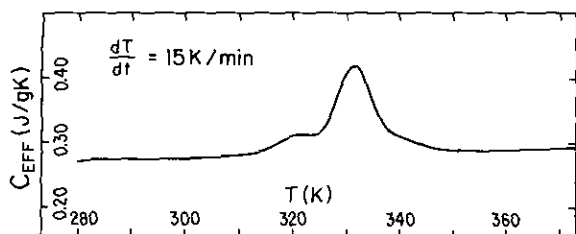


FIG. 4. Differential heat flow, taken with DSC, into a powder from growth-tube-2, converted into an effective specific heat.

ple inhomogeneity (10). The entropy change $\Delta S = \int \Delta C_{\text{EFF}}/T dT \approx 6 \text{ mJ/g}$. The anomaly is double peaked ($\Delta T \approx 10 \text{ K}$).

Superconductivity was investigated for growth-tube-2 material using a low-frequency (14 Hz) ac magnetic susceptibility technique. Sample temperatures were measured using calibrated Ge sensors. The sample was immersed in pumped liquid ^4He for temperatures below 4.2 K. High pressures were generated using a piston-in-cylinder technique (11) with a mixture of 50% isoamyl alcohol and 50% *n*-pentane as a pressure transmitting medium. A high purity lead sample, whose superconducting transition was calibrated as a function of pressure (12), was included in the high pressure environment as a manometer. Pressures were incremented at room temperature.

At ambient pressure, a diamagnetic superconducting onset is observed at 2.3 K, but the diamagnetism is still not saturated at 1.5 K. As the pressure is increased, the onset temperature rapidly increases ($dT_{\text{ON}}/dP \approx 0.13 \text{ K/kbar}$), but the transition remains incomplete above 1.5 K until $\sim 10 \text{ kbar}$. The magnitude of the diamagnetic signal is consistent with bulk superconductivity. The temperature dependence of the diamagnetic signals at three pressures are compared in Fig. 5a, and the temperature dependence of T_{ON} and T_{C} (the midpoint of the inductive transition) is shown in Fig. 5b. As shown, the temperature dependence of T_{C} is somewhat stronger than that of T_{ON} , $dT_{\text{C}}/dP \approx 0.18 \text{ K/bar}$; i.e., the transition becomes sharper with increasing pressure. Checks were also made for pressure hysteresis of T_{C} ; no significant hysteresis could be detected, but the breadth of the transitions makes any such effect difficult to estimate.

DISCUSSION

At the annealing temperature $T_{\text{A}} = 920 \text{ K}$, we obtain the trigonal prismatic polytype, 2H-TaS_2 , when the material is prepared from tantalum foil or wire (7). We suggest that in the present case, the 6R polytype may have been stabilized by the use of partially oxidized tantalum powder as the starting material (7). Hayashi and Kawamura (13) have suggested that for $T_{\text{A}} = 920 \text{ K}$, one obtains the 2H

polytype when using very hydrogenated tantalum, the 6R for intermediate levels of hydrogenation, and 1T when using dehydrogenated tantalum. Perhaps oxygen released from the tantalum powder serves to decrease the hydrogen absorbed in the product. (We note also that no Ta_2O_5 was observed with X-ray diffraction in the product.)

The only previous report of measurements on 6R- TaS_2 was by Thompson (5), who prepared single crystals using phosphorus as a transport agent at 1020 K. He observed two transitions in the *a*-axis resistivity and Hall effect, at 311 and 15 K; only the upper transition (an increase in resistance and Hall constant upon cooling) appeared discontinuous. He measured a temperature independent ($T < 300 \text{ K}$) susceptibility of $0.3 \times 10^{-6} \text{ emu/g}$, 40% larger than our room temperature value, and observed no low-temperature anomaly or ambient pressure superconductivity above 1.7 K.

Thompson (5) compared his results with those obtained for $4\text{H}_b\text{-TaS}_2$ (14), which also has alternating trigonal prismatic and octahedral layers. In the latter polytype, the room temperature susceptibility is $0.21 \times 10^{-6} \text{ emu/g}$, the same as the value we obtain, and has hysteretic and diamagnetic changes (about 10%) upon cooling through 20 and 315 K. The resistance increases discontinuously upon cooling through the upper transition, but decreases at the lower transition. An entropy change of $\Delta S = 6.0$

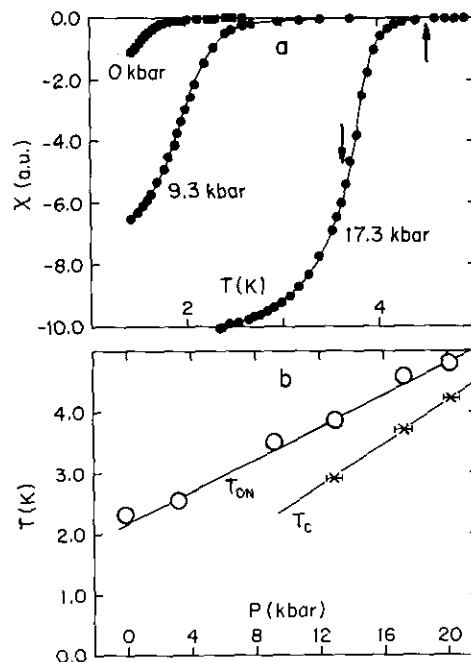


FIG. 5. (a) Temperature dependence of the ac susceptibility of a powder sample (from growth-tube-2) taken at different pressures. The curves are visual guides. The upward and downward arrows for the 17.3 kbar curves define T_{ON} and T_{C} , respectively. (b) The pressure dependence of T_{ON} and T_{C} .

mJ/gK, the same as our value, was observed at the upper transition with DSC; as for our material, the DSC peak for 4H_b-TaS₂ was double, but the peaks were much closer together ($\Delta T = 1$ K) (14) than for our material. No ambient pressure superconductivity was observed above 1.1 K (2).

In comparison, in our material the T_2 transition is at a *much* higher temperature than was previously reported for either the 6R or 4H_b polytype. The magnitudes of the susceptibility changes, however, are similar to those reported for 4H_b-TaS₂ (14). The resistance increases at both T_1 and T_2 transitions.

We note that, like our material, 2H-TaS₂ has a diamagnetic anomaly at 80 K, which is similar in magnitude but very different in shape from ours (15). As discussed above, there is no indication in X-ray diffraction of a significant amount of 2H-TaS₂ in our material. Also, the superconducting transition in 2H-TaS₂ is at 0.8 K (16), much lower than T_{ON} for our compound.

Because the resistance increases and susceptibility decreases on cooling through both the T_1 and T_2 transitions, we suggest that both are charge-density-wave (CDW) transitions (15). The hysteresis in the T_1 transition suggests that it involves a commensurate lock-in (17), presumably on the octahedrally coordinated planes, as suggested for the 4H_b polytype (5, 14), while the closeness to the 2H transition temperature suggests that the T_2 transition is in the trigonal prismatic planes (5, 14). If we associate the susceptibility change at T_1 , $\Delta\chi \approx 2.7 \times 10^{-8}$ emu/g, with a change in Pauli susceptibility, $\Delta\chi = \mu_B^2 \Delta N$, where N is the density of states at the Fermi level, we find the reasonable value $\Delta N \approx 0.20$ states/(eV-molecule). On the other hand, if the observed change in entropy at T_1 is *solely* due to a change in density of states, $\Delta S_{el} \approx (\pi k_B)^2 T_1 \Delta N / 3$, then $\Delta N \approx 2$ states/(eV-molecule). This large discrepancy suggests that the transition entropy also includes a large contribution from phonons, due to a very small CDW coherence length (i.e., strong coupling) (18), as is known to occur for 2H-TaSe₂. For 2H-TaSe₂, however, the transition (into an incommensurate, but nearly commensurate, CDW state) is second order (18, 19).

As mentioned above, two peaks are observed in c_{EFF} near T_1 , suggesting that there are in fact two transitions. The upper peak coincides with the susceptibility maximum and the lower peak with the shoulder in the susceptibility (see Fig. 2). Alternatively, the large width and structure at this transition may indicate that the CDW state is disordered.

The large enhancement of the superconducting transition temperature with pressure is consistent with the existence of one or more CDW states. The latter are usually suppressed by pressure, increasing the area of Fermi surface available for formation of superconducting Cooper pairs (20, 21). Incomplete, or very broad, superconducting transitions have previously been observed in some transi-

tion metal chalcogenides with coexisting CDWs (16, 20–22). An unknown, or mixed, polytype of TaS₂ prepared at 980 K had a superconducting onset at 2.1 K, close to our value; the large width (>0.5 K) of the transition was attributed to *excess tantalum* (22). On the other hand, DiSalvo *et al.* felt that the broad transition in 2H-TaS₂ ($T_{ON} = 0.8$ K) was intrinsic to the stoichiometric material (16). In our case, the fact that the transition sharpens with increasing pressure suggests that its width is affected by the CDW, or perhaps disorder in the CDW. (However, similar sharpening of the superconducting transition with pressure was observed for NbSe₃ (20), which has an extremely well-ordered CDW.)

In conclusion, three phase transitions are observed in powders of 6R-TaS₂. Two transitions, involving increases in resistance and decreases in susceptibility, are observed at 325 and 80 K. These are tentatively interpreted as CDW transitions. Superconductivity is observed with an ambient pressure onset of 2.3 K, higher than previously observed for any TaS₂ polytype; the strong pressure dependence of the transition is consistent with the suppression of the CDW with pressure. These properties differed from those previously reported (5), indicating their strong dependence on various defects which may result from different growth conditions.

ACKNOWLEDGMENTS

We thank F. J. DiSalvo for helpful comments, M. Chung for technical assistance, and M. Blauvelt and H. Mefford for designing and constructing the pellet die, piston, and anvil. This research was supported in part by U.S. National Science Foundation Grant EHR-9108764.

REFERENCES

1. J. A. Wilson and A. D. Yoffe, *Adv. Phys.* **73**, 193 (1969); R. M. A. Lieth and J. C. Terhell, in "Preparation and Crystal Growth of Materials with Layered Structures" (R. M. A. Lieth, Ed.), p. 141. Reidel, Dordrecht, 1977.
2. S. F. Meyer, R. E. Howard, G. R. Stewart, J. V. Acrivos, and T. H. Geballe, *J. Chem. Phys.* **62**, 4411 (1975).
3. R. H. Friend and A. D. Yoffe, *Adv. Phys.* **36**, 1 (1987).
4. F. Jellinek, *J. Less-Common Met.* **4**, 9 (1962).
5. A. H. Thompson, *Solid State Commun.* **17**, 1115 (1975).
6. F. Hulliger, in "Structural Chemistry of Layer-Type Phases" (F. Levy, Ed.), p. 241. Reidel, Dordrecht, 1976.
7. F. J. DiSalvo, private communication.
8. Y. Wang, M. Chung, T. N. O'Neal, and J. W. Brill, *Synth. Met.* **46**, 307 (1992).
9. G.-W. Jang and K. Rajeshwar, *Anal. Chem.* **58**, 416 (1986).
10. M. Chung, E. Figueroa, Y.-K. Kuo, Y. Wang, J. W. Brill, T. Burgin, and L. K. Montgomery, *Phys. Rev. B* **48**, 9256 (1993).
11. P. E. Chester and G. O. Jones, *Phil. Mag.* **44**, 1281 (1953).
12. T. F. Smith, C. W. Chu, and M. B. Maple, *Cryogenics* **9**, 53 (1969).
13. K. Hayashi and A. Kawamura, *Mater. Res. Bull.* **21**, 1405 (1986).
14. F. J. DiSalvo, B. G. Bagley, J. M. Voorhoeve, and J. V. Waszczak, *J. Phys. Chem. Solids* **34**, 1357 (1973).
15. J. A. Wilson, F. J. DiSalvo, and S. Majahan, *Adv. Phys.* **24**, 117 (1975).

16. F. J. DiSalvo, R. E. Schwall, T. H. Geballe, F. R. Gamble, and J. H. Osiecki, *Phys. Rev. Lett.* **27**, 310 (1971).
17. W. L. McMillan, *Phys. Rev. B* **14**, 1496 (1976).
18. W. L. McMillan, *Phys. Rev. B* **16**, 643 (1977).
19. R. A. Craven and S. F. Meyer, *Phys. Rev. B* **16**, 4583 (1977).
20. M. Ido, Y. Okayama, T. Ijiri, and Y. Okajima, *J. Phys. Soc. Jpn.* **59**, 1341 (1990).
21. M. Nunez-Regueiro, J.-M. Mignot, M. Jaime, D. Castello, and P. Monceau, *Synth. Met.* **55-57**, 2653 (1993).
22. M. H. Van Maaren and G. M. Schaeffer, *Phys. Lett. A* **24**, 645 (1967).